Biodegradation (2006) 17: 423–435
DOI 10.1007/s10532-005-9013-y

Influence of a nonaqueous phase liquid (NAPL) on biodegradation of phenanthrene

T.R. Sandrin[1], W.B. Kight[2], W.J. Maier[2] & R.M. Maier[2,*]
[1]*Department of Biology and Microbiology, The University of Wisconsin Oshkosh, Oshkosh, WI 54901, USA;*
[2]*Department of Soil, Water and Environmental Science, The University of Arizona, Shantz Building #38 , Tucson, AZ 85721, USA (*author for correspondence: e-mail: rmaier@ag.arizona.edu)*

Accepted 8 August 2005

Key words: biodegradation, hexadecane, modeling, NAPL, phenanthrene

Abstract

A series of batch reactor experiments was carried out to examine the effect of a nonaqueous phase liquid (NAPL) on the biodegradation of a hydrophobic solute. A mathematical program model that describes physical processes of solute solubilization and partitioning between the NAPL and aqueous phases as well as microbial degradation and oxygen utilization was used to analyze the test data. The model calculates the cumulative changes in concentration of substrate, cell mass, carbon dioxide, and dissolved oxygen as a function of time. The equations incorporate the effects of solute solubilization, partitioning, biodegradation, as well as oxygen availability. Hexadecane was used as the model NAPL and was not biodegraded in the timeframe of the experiments performed. The model solute was the polyaromatic hydrocarbon, phenanthrene. In agreement with several previous studies, experimental measurements showed that hexadecane increased rates of mineralization of 15 mg phenanthrene when present at low mass but decreased rates at high mass. Model results suggest that partitioning of the phenanthrene into the hexadecane phase limits bioavailability at high NAPL mass. Further the model suggests that mineralization rates were higher with the low NAPL mass because aqueous phenanthrene concentrations were higher in those treatments from ca. 20 to 40 h than in other treatments. Finally, experiments showed that the presence of hexadecane, at all masses tested, resulted in a lower cell yield, effectively increasing the amount of CO_2 produced during the experiment. Model results suggest that this is due to changes in phenanthrene metabolism that are induced by the presence of the hexadecane phase. Model studies aimed at increasing rates of biodegradation by modifying operating conditions are described along with practical approaches to implementing these modifications.

Introduction

Remediation of polyaromatic hydrocarbon (PAH) contaminated sites is often complicated by the presence of a nonaqueous phase liquid (NAPL). In this type of multiphase system, it has been observed that the NAPL can inhibit PAH biodegradation (Birman & Alexander 1996; Carroquino & Alexander 1998; Efroymson & Alexander 1994, 1995; Fu & Alexander 1995; Gamerdinger et al. 1995; Labare & Alexander 1995). The mechanism of inhibition may involve one or both of the following: (1) reduced bioavailability of the PAH due to its partitioning from the aqueous phase into the NAPL phase (Efroymson & Alexander 1995), and (2) competition between biodegradation requirements of the PAH and NAPL for inorganic nutrients such as oxygen, nitrogen, and phosphorous (Morrison & Alexander 1997).

Efroymson & Alexander (1994, 1995) proposed that partitioning reduces aqueous phase PAH concentrations below a threshold level required for

biodegradation. In support of this, Ortega-Calvo et al. (1995) found that rates of mineralization of PAH in a NAPL increased as partitioning rates of the PAH from the NAPL increased. Partitioning rates were affected by the type of NAPL used and whether the system was shaken. Despite the correlation between partitioning and mineralization rates, several studies have shown that maximum biodegradation rates cannot be predicted on the basis of partitioning alone (Carroquino & Alexander 1997; Efroymson & Alexander 1994; Garcia-Junco et al. 2001; Ortega-Calvo et al. 1995).

Competition between a NAPL and PAH for oxygen and inorganic nutrients required for biodegradation may be another cause of inhibition. For example, phenanthrene biodegradation was inhibited in the presence of a biodegradable NAPL as a result of reduced oxygen tension (Morrison & Alexander 1997). Oxygen limitations were not imposed by a nonbiodegradable NAPL. The addition of nitrogen and phosphorous to soil and aquifer solids increased mineralization rates of di(2-ethylhexyl) phthalate dissolved in a variety of NAPLs (Labare & Alexander 1995). Similarly, phenanthrene biodegradation in the presence of biodegradable NAPL (hexadecane, dodecane) was increased by adding nitrogen and phosphorous (Morrison & Alexander 1997).

These studies have provided valuable qualitative insights into the possible mechanisms involved in biodegradation of solutes such as PAH in multiphase systems. The rationale for the work described here is to provide quantitative information that can be used to describe the critical process variables that are affected by the presence of NAPL. Such quantitative information is needed to evaluate: (i) PAH movement within a contaminated site, (ii) PAH remediation outcomes especially for monitored natural attenuation and, (iii) appropriate remediation strategies. The objective of this work is to quantitatively examine the influence of a model NAPL on the fate and behavior of a solute in a multiphase system using a combined experimental and modeling effort. A set of experiments was performed using phenanthrene as the representative PAH and hexadecane as a representative NAPL, in this case one that is less dense than water. A *Burkholderia cepacia* isolate that could degrade phenanthrene, but not hexadecane during the time course of the experiments described here, was used to evaluate phenanthrene biodegradation. A model was developed to simulate the physical processes of solute solubilization and partitioning in the presence of a NAPL, as well as the biological processes of solute and oxygen utilization. The model was calibrated using the experimental biodegradation data and then used to explore the fate of the solute in the aqueous-NAPL system. In addition, the model contains several user-specified parameters (e.g., interfacial area, substrate inhibition, biodegradation of the NAPL phase) that ensure that the model is broadly applicable to other aqueous-NAPL systems.

Materials and methods

Model phenanthrene degrader

Burkholderia cepacia CRE7 was chosen because it utilizes phenanthrene as a sole source of carbon and energy following a short lag phase, ca. 5 h. CRE7 also mineralizes hexadecane, but only following a lag phase of 150 h which was the limit of the experiments performed in this study. A lyophilized culture of CRE7 was inoculated into a 125 ml flask containing 30 ml mineral salts broth (MSB) and 15 mg phenanthrene. After incubation at 25 °C for 48 h at 200 rpm, this culture was plated on MSA-phenanthrene plates. The MSA-phenanthrene plates (15 g purified agar/l) were prepared from a MSB adjusted to pH 7.2 and containing per liter: KH_2PO_4 (1 g), Na_2HPO_4 (1 g), NH_4NO_3 (0.5 g), $(NH_4)_2SO_4$ (0.5 g), $MgSO_4 \cdot 7H_2O$ (0.2 g), $CaCl_2 \cdot 2H_2O$ (0.02 g), $FeCl_3$ (0.002 g), and $MnSO_4 \cdot 2H_2O$ (0.002 g). A 500 mg/l phenanthrene solution was prepared in chloroform and 0.5 ml was added to each plate. The chloroform was evaporated, leaving 0.25 mg of phenanthrene on each plate. The culture was transferred monthly for the duration of this study. Prior to each experiment, a preculture was prepared by inoculating a colony from an MSA-phenanthrene plate into 30 ml MSB containing 15 mg phenanthrene. This preculture was incubated for 24 h at 25 °C at 200 rpm. A second preculture was inoculated and incubated under the same conditions. Finally, 1.0 ml from the second preculture containing ca. 5×10^6 CFU was used to inoculate experimental flasks.

Phenanthrene and hexadecane biodegradation

Mineralization of [9-^{14}C] phenanthrene (8.5 mCi/mmol, >98% purity; Sigma Chemical Co.) was measured to determine the effect of a NAPL (hexadecane) on the kinetics of phenanthrene biodegradation by CRE7. Experiments were performed in triplicate in 250 ml screwcap flasks fitted with caps modified for atmospheric evacuation. The bottom of each flask was coated with 1.5 or 15 mg phenanthrene containing approximately 0.03 μCi [9-^{14}C] phenanthrene that was prepared as follows. Phenanthrene (75 mg or 750 mg) was dissolved in 10 ml dichloromethane and then spiked with 15 μl of ^{14}C-phenanthrene (specific activity = 0.1 μCi/μl). A 0.2 ml aliquot of one of these solutions was placed into each 250 ml flask and the dichloromethane was allowed to evaporate overnight in a fume hood. Hexadecane was then added to attain phenanthrene:hexadecane mass ratios of 1:0, 1:20, 1:200, and 1:2000. MSB (29 ml) and 1 ml inoculum ($\sim 5 \times 10^6$ CFU/ml) was added to each flask Flasks were incubated at 25 °C at 200 rpm. Periodically, the atmosphere in each flask was evacuated and $^{14}CO_2$ was collected using a flushing tree (Marinucci & Bartha 1979). Radioactivity was determined using a liquid scintillation counter (1600 TR, Packard Instrument Company, Meridian, CT). Rates of phenanthrene biodegradation in experiments were calculated by determining the slope of the linear portion of the mineralization curves. For experiments using 1.5 mg phenanthrene, rates were calculated from 14 to 25 h. For experiments using 15 mg phenanthrene, rates were calculated from 20 to 37 h. We quantified total phenanthrene mineralization at 111 h.

Hexadecane mineralization was also evaluated in this system to determine the onset and extent of its mineralization in comparison to phenanthrene mineralization. Triplicate experimental flasks were constructed as described above except unlabeled phenanthrene and [1-^{14}C] hexadecane were used (0.045 μCi/flask).

Dissolved oxygen concentrations

To determine whether hexadecane reduced dissolved oxygen (DO) concentrations in the aqueous phase of experimental flasks during mineralization, an identical experiment was performed except that neither the phenanthrene nor the hexadecane was radiolabeled. The DO concentration in the aqueous phase of each flask was determined by placing an oxygen microelectrode (Microelectrodes Inc., Bedford, NH) into the aqueous phase below the NAPL layer. To avoid contamination of this system, DO concentrations were determined at a single time point: 48 h after inoculation when phenanthrene degradation rates were highest and oxygen limitations would be expected to be greatest.

Mass distribution of phenanthrene

To determine the phase distribution (aqueous phase, NAPL phase, solid dispersed phase, or solid sorbed phase) of phenanthrene prior to inoculation, triplicate flasks were amended with 1.5 mg of [9-^{14}C] phenanthrene, 0, 30, 300, or 3000 mg unlabeled hexadecane, and 30 ml MSB as described above. After 0.75 h of agitation at 200 rpm, 20 ml of the aqueous phase was removed and passed through a glass syringe packed with glass wool to remove suspended (dispersed) phenanthrene crystals. Triplicate 1 ml samples of the aqueous filtrate were analyzed for radioactivity to determine the aqueous phase concentration of phenanthrene. The column was then rinsed with 40 ml of dichloromethane and triplicate 1 ml dichloromethane samples were analyzed for radioactivity to determine the dispersed solid phase phenanthrene. For treatments containing 300 and 3000 mg hexadecane, triplicate 20 μl samples of the hexadecane phase remaining in each flask were carefully removed and analyzed for radioactivity to determine the amount of phenanthrene partitioned into the NAPL phase. This analysis could not be performed on the 30 mg treatment since there was too little hexadecane to allow recovery. Finally, the remaining contents of the flask (aqueous, hexadecane, and sorbed phenanthrene phases) were extracted with 20 ml of dichloromethane and triplicate 1 ml samples of the dichloromethane were analyzed for radioactivity. The sorbed solid phase phenanthrene in the system was then determined by subtracting the amount of phenanthrene contained in the hexadecane and aqueous phases from the total amount of phenanthrene obtained in the extraction (Table 1).

Table 1. Effect of NAPL mass on distribution of 1.5 mg phenanthrene in a multiphase system

NAPL mass (mg)	Phenanthrene (%)			
	Aqueous phase	NAPL phase	Solid phase dispersed	Solid phase (flask bottom)
0	0.05 ± 0.05	–	2.8 ± 2.2	97 ± 6.2
30	0.17 ± 0.10	ND	1.3 ± 0.17	99 ± 4.8
300	0.16 ± 0.014	4.3 ± 5.1	0.97 ± 0.63	95 ± 8.8
3000	0.05 ± 0.007	99 ± 3.0	0.70 ± 0.23	0 ± 0

Values are means and standard deviations of triplicate flasks. ND is not determined.

Mathematical model

A computer program was used to simulate the physical-chemical-biological reactions involved in biodegradation of solid phase phenanthrene in the presence of hexadecane (Jahan et al. 1999; Papageorgakopoulou & Maier 1984). This program is written for systems containing both a biodegradable solute and NAPL. However, in this study, biodegradation of the NAPL phase did not occur within the timeframe of the experiments, therefore, the governing equations presented describe only solute biodegradation. The governing equations (constant definitions are presented in Table 2) used in BRKNAPL are as follows:

Equations 1 and 2 represent the active cell mass balance where microbial growth is described using a modified Monod equation that incorporates the effect of time-dependent DO changes. The cumulative cell mass concentration is adjusted for endogenous metabolism using a first order rate equation.

$$\frac{dX_1}{dt} = A_1 - \frac{dX_{1,\text{initial}}}{dt} - kd \times X_1 \tag{1}$$

$$A_1 = \frac{(\mu_1 \times C_1 \times X_1)}{Ksc_1 + C_1 + \frac{C_1}{Ki,1}} \times \frac{\text{DO}}{(Ks_{\text{DO}} + \text{DO})} \tag{2}$$

A_1 (see Equation 2) describes the dependence of growth on substrate (phenanthrene) concentration, maximum growth rate, the active cell mass, the half saturation constant, an inhibition coefficient, and oxygen availability.

An initial lag phase effect can also be incorporated (Equation 3) :

$$\frac{dX_{1,\text{initial}}}{dt} = -(ka_1 \times t^m \times X_{1,\text{initial}}) \tag{3}$$

Equation 4 describes the changes in phenanthrene concentration versus time. In this study the NAPL [hexadecane] concentration was assumed to be constant and dissolution into the water phase was neglected. Both kL_1 and KSA_1 are empirical parameters that are specific to test conditions, such as intensity of mixing/agitation and the surface area of contact between the NAPL and water phase. For these experiments, the initial phenanthrene mass was present as a solid phase sorbed to the bottom of the flask and subject to solubilization into the aqueous phase and subsequent partitioning between the aqueous and hexadecane phases. The interfacial surface area of the solid phase phenanthrene (KSA_1) is expressed in terms of surface area per unit mass which allows adjustment of the surface area to reflect residual phenanthrene concentration as a function of time. This is done using the exponent "n" which characterizes the change in interfacial surface area as the mass of Cxs_1 decreases with time.

$$\frac{dCxs_1}{dt} = -kL_1 \times (KSA_1 \times Cxs_1 0^n \times Cxs_1^{(1-n)}) \times (Cs_1 - C_1) \tag{4}$$

Equation 5 represents partitioning of soluble phenanthrene between the NAPL and water phases where $C_{1,\text{NAPL}}$ represents the concentration of C_1 partitioned into the NAPL phase and KSA_2 is a measure of the surface area interface between the water and NAPL phases. In this study, hexadecane is treated as a liquid phase floating on the aqueous phase; however, users can also apply the model to systems containing NAPL droplets by adjusting the value of the NAPL-aqueous phase interfacial area parameter (KSA_2) accordingly.

$$\frac{dC_{1,\text{NAPL}}}{dt} = -kc_{1,\text{NAPL}} \times (KSA_2 \times Cxs_2 0^n \times Cxs_2^{(1-n)}) \times (C_{1,\text{film}} - C_1) \tag{5}$$

In Equation 5, $C_{1,\text{NAPL}}$ represents the concentration of phenanthrene that is partitioned/dissolved in the NAPL phase. Partitioning is described by a

Table 2. Model constants and variables

Constant/variable	Description	Base case value[b]
C_1	Aqueous phase concentration of phenanthrene (M V^{-1})	0.0001
Cxs_1	Mass of solid phase phenanthrene (M V^{-1})	48.4
Cxs_2	Mass of NAPL added (M V^{-1})	0.0[a]
DO	Aqueous DO concentration (M V^{-1})	8.0
CO_2	CO_2 produced (M V^{-1})	0.0
$C_{1,NAPL}$	Phenanthrene partitioned into the NAPL phase (M V^{-1})	0.0
X_1	Actively biodegrading population (M V^{-1})	0.0
Xin_1	Inactive biodegrading population (M V^{-1})	0.45
t	Time (T)	0.0
Y	Cell mass yield constant (M M^{-1})	1.0
$Y_{gr,1}$	Growth related oxygen utilization constant (M M^{-1})	1.54
Y_{end}	Endogenous oxygen utilization constant (M M^{-1})	1.98
YCO_2	Growth related CO_2 production constant (M M^{-1})	1.26
$YCO_{2,end}$	CO_2 from endogenous metabolism constant (M M^{-1})	1.95
Ks_1	Half saturation constant for phenanthrene (M V^{-1})	0.0005
Ki_1	Substrate interaction/inhibition constant (M V^{-1})	100,000
Ks_{DO}	Half saturation constant for oxygen (M V^{-1})	1.0
Cs_1	Saturated aqueous phenanthrene concentration (M V^{-1})	1.12
DO_s	Saturation solubility of DO (M V^{-1})	8.0
m	Activation process exponent	1.0
n	Cxs exponent that controls changes in KSA	−0.1
kL_1	Solid phase solute dissolution rate constant (T^{-1} A^{-1})	100.0
KSA_1	interfacial surface area of phenanthrene (A M^{-1})	0.0008
KSA_2	Interfacial surface area of hexadecane (A M^{-1})	–
KLA	Oxygen dissolution rate constant (T^{-1})	2.0
$kc_{1,NAPL}$	Departitioning rate constant C_1 from Cxs_2 (T^{-1} A^{-1})	–
ka_1	Cell mass activation rate constant (T^{-2})	1.0
μ_1	Growth rate constant (T^{-1})	0.35
kd	Endogenous rate constant (T^{-1})	0.0005

[a]The program requires that a very small but finite value be used.
[b]The base case assumed 1.5 mg phenanthrene and no hexadecane.

mass transport equation that includes a mass transfer coefficient ($kc_{1,NAPL}$), a parameter that characterizes the interfacial surface area of the NAPL phase (KSA_2, the surface area per unit mass of hexadecane), and a term that describes equilibrium partitioning of dissolved phenanthrene using a modification of Raoult's Law. It is postulated that $C_{1,NAPL}$ dissolves back into the water phase as the concentration of C_1 decreases due to biodegradation. Solubilization is assumed to be driven by the concentration difference $C_{1,film} - C_1$. $C_{1,film}$ represents the concentration of C_1 in the stagnant water film on the surface of Cxs_2. It is assumed to be in equilibrium with $C_{1,NAPL}$ which implies that dissolution into the water film is relatively fast whereas transport from the film into the water phase is the rate-limiting process. Based on Raoult's Law, the equilibrium concentration of C_1 in the film should be dependent on the mole fraction of chemical in the Cxs_2 phase. The Raoult's Law effect has been approximated to simplify the model by using a mass fraction because the moles of $C_{1,NAPL}$ are much smaller than the moles of the Csx_2 phase and molecular weights of the two chemicals are in the same range, thus $C_{1,film} = C_{S1} \times C_{1,NAPL}/Cxs_2$. Incorporation of the Raolt's Law modification results in Equation 6:

$$\frac{dC_{1,NAPL}}{dt} = -kc_{1,NAPL} \times (KSA_2 \times Cxs_2 0^n \times Cxs_2^{(1-n)}) \times (Cs_1 \times \frac{C_{1,NAPL}}{Cxs_2} - C_1) \quad (6)$$

Equation 7 represents the aqueous phase phenanthrene concentration which is calculated from the time dependent changes in dissolution of the solid

phase, partitioning between water and NAPL phases, and biodegradation.

$$\frac{dC_1}{dt} = -\frac{dCxs_1}{dt} - \frac{dC_{1,\mathrm{NAPL}}}{dt} - \frac{A_1}{Y_1} \tag{7}$$

Equation 8 represents the change in DO concentration as a function of time. This equation includes the classical rate equation $kLA\times(\mathrm{DO_s} - \mathrm{DO})$ that describes reaeration of the water phase. It also includes description of the rate of oxygen utilization for growth and endogenous metabolism.

$$\frac{d\mathrm{DO}}{dt} = kLA \times (\mathrm{DO_S} - \mathrm{DO}) - Y_{\mathrm{gr},1} \times A_1 - Y_{\mathrm{end}} \times kd \times X_1 \tag{8}$$

Equation 9 represents cumulative carbon dioxide production which is calculated from a carbon dioxide mass balance that describes mineralization associated with growth of cell mass and endogenous decay of cell mass using carbon dioxide yield coefficients for cell growth and for endogenous metabolism.

$$\frac{d\mathrm{CO}_{2,1}}{dt} = A_1 \times Y\mathrm{CO}_{2,1} + kd \times X_1 \times Y\mathrm{CO}_{2,\mathrm{end}} \tag{9}$$

Results and discussion

Phenanthrene biodegradation in the presence and absence of NAPL

Mineralization of phenanthrene by CRE7 in the absence of NAPL was approximately 35% representing 60 and 600 mg CO_2/l for the 1.5 and 15 mg phenanthrene treatments respectively (Figure 1a, b). Mineralization plateaued before 150 h, the lag phase for onset of NAPL mineralization supporting the assumption that only phenanthrene biodegradation was occurring. This was confirmed by a separate experiment performed under identical conditions except that the hexadecane was radiolabeled instead of the phenanthrene (data not shown).

NAPL addition impacted both the rate and extent of phenanthrene mineralization. This can be best seen at the higher level of phenanthrene tested, 15 mg (Figure 1b). The 20:1 NAPL treatment exhibited a mineralization rate of 20 mg CO_2/l/h which is significantly higher than the rates for 200:1 NAPL and no NAPL treatments which were similar at 9.3 and 8.6 mg CO_2/l/h. The 2000:1 NAPL treatment exhibited the lowest mineralization rate, 1.6 mg CO_2/l/h. In terms of extent of mineralization, comparison of the three treatments that plateaued at 111 h shows that the greatest extent of mineralization was exhibited by the 20:1 treatment (780 mg CO_2/l). Significantly lower levels were exhibited by the 200:1 NAPL and no NAPL treatments (540 and 580 mg CO_2/l respectively). For the 1.5 mg phenanthrene experiments (Figure 1a), rates of mineralization among treatments followed a pattern similar to that observed for the 15 mg phenanthrene experiments. The highest rate of 4.8 mg CO_2/l/h was observed for the 20:1 NAPL treatment. Rates were similar for the 200:1 and no NAPL treatments (2.9 mg CO_2/l/h) and was lowest for the 2000:1 NAPL treatment (0.7 mg CO_2/l/h). There was no significant difference at 111 h in the extent of mineralization among the four treatments. However, the trend in the data suggests that the highest extent of mineralization was reached in the 20:1 and 200:1 NAPL treatments (82 and 78 mg CO_2/l respectively). Mineralization reached 65 and 59 mg CO_2/l for the no NAPL and 2000:1 NAPL treatments respectively.

Similar inhibitory (Birman & Alexander 1996; Carroquino & Alexander 1998; Fu & Alexander 1995; Morrison & Alexander 1997) and stimulatory effects of NAPL phases on PAH biodegradation have been reported (Jimenez & Bartha 1996; Kanaly et al. 2000, 2001; Kohler et al. 1994). In addition, at least one study has reported no effect of a transformer oil NAPL on the extent of phenanthrene mineralization (Doick & Semple 2003). In looking more closely at the cases of inhibition, it has been suggested that the presence of a large amount of NAPL phase reduces the bioavailability of the target substrate (Efroymson & Alexander 1995), or that availability of oxygen or nutrients is limited (Morrison & Alexander 1997). However, there has been no quantitative description of the physical and biological mechanisms that are involved. A detailed analysis of the experimental data was therefore carried out using BRKNAPL to simulate the mineralization observed in all eight experiments shown in Figure 1. This allowed us to determine the quantitative changes in process variables that were necessary as

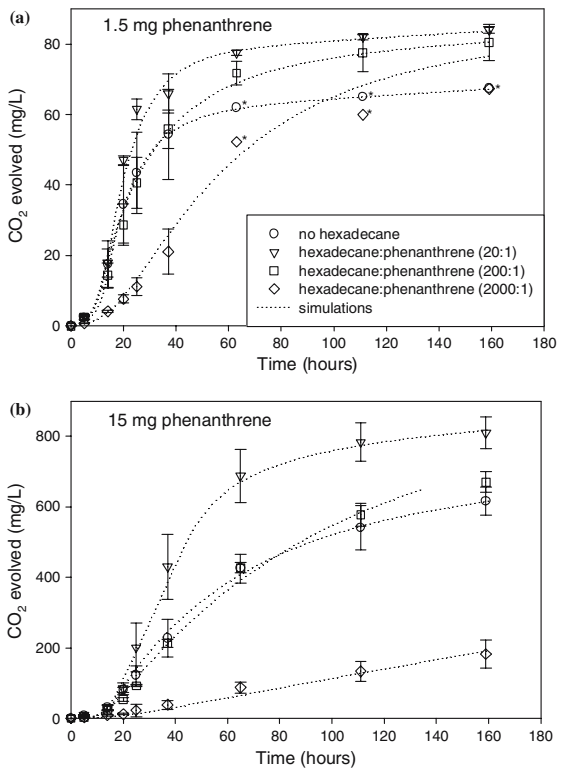

Figure 1. Mineralization of phenanthrene in the presence and absence of a hexadecane NAPL phase. The symbols represent means and standard deviations of triplicate experimental data points and the dotted lines represent model simulations. (a) The mass of phenanthrene added was 1.5 mg. The mass of hexadecane added was 0, 30, 300, or 3000 mg. (b) The mass of phenanthrene added was 15 mg. The mass of hexadecane added was 0, 300, 3000, or 30,000 mg. Note that for (a) standard deviations are not given for the six points with stars next to them. This is because the standard deviations were large and obscured the comparison of the data points with the modeling lines. The relevant data and standard deviations are as follows: no hexadecane 63 h, 62.0 ± 13.5; 111 h, 65.1 ± 13.7; 159 h, 67.5 ± 12.4; hexadecane:phenanthrene 2000:1 63 h, 52.2 ± 20.5; 111 h, 60.0 ± 27.6; 159 h, 67.3 ± 21.8 mg CO_2/l.

NAPL:phenanthrene ratios were changed. These process variables characterize bioavailability, growth kinetics, and oxygen availability during mineralization of phenanthrene in each system.

Model calibration

Table 2 lists all of the model parameters along with the initial values for fitting the "base case" test data (1.5 mg phenanthrene, no hexadecane). Most of the values were determined from independent literature data sources, for example, parameters related to growth metabolism, endogenous metabolism, oxygen utilization, and re-aeration. The exceptions are discussed below.

Simulations of phenanthrene mineralization in the absence of NAPL

Measured and simulated mineralization data for 1.5 and 15 mg phenanthrene are in good agreement (Figure 1a, b). Simulations of the test data required changing the values of two parameters, namely Cxs_1, the mass of solid phase phenanthrene coated on the bottom of the flask and KSA_1, the surface area of phenanthrene exposed to the water phase. The initial value of Cxs_1 was calculated from the mass of phenanthrene added to each flask but the decrease in Cxs_1 was calculated by the model. KSA_1, which describes the interfacial area between the phenanthrene and water phases (area/mass of phenanthrene), was fitted by the model with initial values of 0.0008 and 0.00019 cm^2/mg for 1.5 and 15 mg phenanthrene respectively. Independent measurements of the surface area of the phenanthrene phase on the flask bottom were essentially the same (data not shown). The lower KSA_1 value for 15 mg is consistent with the observation that the surface area of the coating did not increase in proportion to the increase in mass implying that phenanthrene was deposited as a thicker layer. Additional simulations were generated to examine the sensitivity of mineralization to changes in KSA_1, keeping all other parameters constant. For example, lowering the value of KSA_1 by 50% reduced the rate of mineralization by 65% during the exponential growth phase whereas doubling KSA_1 increased the rate of mineralization by 30%. These results indicate that the interfacial area between the water and phenanthrene phases is a rate-limiting factor even though phenanthrene is eventually metabolized given enough time (data not shown).

Effect of hexadecane (NAPL) addition

Experimental data for the 1.5 and 15 mg phenanthrene experiments in the presence of NAPL were reasonably well-fitted by the computer simulations for all levels of NAPL tested. Simulating mineralization in the presence of NAPL required specifying four additional parameters: Cxs_2, the concentration of NAPL added; KSA_2, the area of

contact between the NAPL and aqueous phases; $C_{1,NAPL,initial}$, the initial mass of phenanthrene partitioned into the NAPL phase before inoculation; and $kc_{1,NAPL}$, the mass transfer coefficient for phenanthrene between the aqueous and NAPL phases. Values for Cxs_2 and KSA_2 were calculated from the mass of NAPL added and the dimensions of the flasks. Initial values for $C_{1,NAPL,initial}$ were measured independently for each level of NAPL added (Table 1). However, the changes in $C_{1,NAPL}$ with time were calculated by the model. The value of $kc_{1,NAPL}$, which defines the partitioning rate for phenanthrene between the NAPL and aqueous phases, was fitted because partitioning rates were not measured independently. Simulations show that the best fit values of $kc_{1,NAPL}$ decreased as the NAPL phase mass was increased. This indicates that the phenanthrene partitioning rate into and out of the NAPL phase decreases as the NAPL mass is increased (Table 3). This behavior can be ascribed to the fact that, in our flask system, increasing the NAPL increased its volume without increasing the surface area (i.e., NAPL covered the entire surface of the aqueous phase and addition of more NAPL merely increased the thickness of the NAPL phase).

All the model simulations of CO_2 production in the presence of NAPL utilized lower values of the cell mass yield coefficient (Y) and higher values of the CO_2 yield coefficient YCO_2 to fit the data (Table 3). These changes in Y and YCO_2 are consistent with the experimental finding that the amount of CO_2 produced was greater in the presence of NAPL (Figure 1 a, b). YCO_2 is used in BRKNAPL to calculate mineralization as a function of time from the corresponding incremental increase in cell mass. However, Y and YCO_2 are related in the sense that their combined value is constrained by carbon mass balance considerations and thus, increasing YCO_2 requires decreasing Y. In the model, the relationship between Y and YCO_2 for phenanthrene biodegradation was calculated using a carbon mass balance that assumes: (i) the cell mass composition is given by $C_5H_7NO_2$, (ii) that CO_2 is the only other carbon-containing byproduct of metabolism, and (iii) that phenanthrene is completely degraded. As indicated in Table 3, all the simulations that included NAPL were fitted using the same values for Y (0.85) and YCO_2 (1.86) indicating that these values are independent of the NAPL mass added (in the range 30 to 30,000 mg tested). These values can be compared to those used for phenanthrene in the absence of NAPL, 1.0 and 1.26 for Y and YCO_2 respectively. In this case, the Y value (1.0) was obtained from measurements reported in the literature (Woo & Rittman 2000; Zhang et al. 1997) and the YCO_2 value was fitted.

The model simulations indicate that only the presence of NAPL, not the mass and volume of the NAPL phase affected Y and YCO_2. This suggests that it is the aqueous phase and not the NAPL phase of hexadecane that alters metabolism and results in changes in the Y and YCO_2 values. This line of reasoning leads to the idea that changes in metabolism are induced by the presence of soluble or colloidal dispersions of hexadecane. The aqueous solubility of hexadecane in water is low (0.006 mg/l) but under the conditions of these experiments, wherein the flasks were shaken, in addition to the soluble hexadecane, there were likely colloidal dispersions of hexadecane in the aqueous phase. Thus, it is possible that dispersed/soluble hexadecane alters the cell uptake of phenanthrene resulting in an expenditure of additional energy for cell growth resulting in greater CO_2 production. This could be manifested as physiological changes induced by hexadecane to prepare for mineralization which commenced at approximately 150 h. Alternatively, this could be due to hexadecane-induced cell surface changes that impacted the uptake of phenanthrene. For example, there have been several reports describing the ability of NAPL, hydrophobic solutes, and secondary metabolites, such as biosurfactants, to alter cell surface properties which in turn, impacts the biodegradation of both soluble and slightly soluble substrates (Al-Tahhan et al. 2000; Prabhu & Phale 2003; Zhang & Miller 1994).

Effect of oxygen availability

BRKNAPL calculates DO concentrations in the water phase through a mass balance between oxygen utilization (bacterial growth and endogenous metabolism) and aeration from the overlying air phase. Initial DO concentrations were set at 8 mg/l (air saturation) and the effect of DO on cell growth was incorporated into the Monod growth function using a half saturation constant of 1.0 mg/l.

Table 3. Values of $kc_{1,NAPL}$ and YCO_2 used in model simulations

Hexadecane (mg)	1.5 mg Phenanthrene			15 mg Phenanthrene		
	$kc_{1,NAPL}$	Y	YCO_2	$kc_{1,NAPL}$	Y	YCO_2
0	0	1.0	1.26	0	1.0	1.26
30	150	0.85	1.86	–	–	–
300	50	0.85	1.86	150	0.85	1.86
3000	25	0.85	1.86	20	0.85	1.86
30000	–	–	–	3	0.85	1.86

In simulations of the 1.5 mg phenanthrene tests, DO concentrations decreased only very slightly, down to 6 mg/l, during the first 20 h and then rebounded to ambient levels suggesting that oxygen was not limiting either in the absence or presence of a NAPL phase (Figure 2a). These results are confirmed by an oxygen electrode measurement made at 48 h which showed no decrease in DO levels. For the 15 mg phenanthrene tests, simulations show larger decreases in DO, to less than 1 mg/l by 20 h which rebounded to ambient levels as biodegradation reached stationary phase (Figure 2b). As hexadecane in the system is increased (200:1 and 2000:1), the reduction in DO becomes smaller (Figure 2b) because rates of biodegradation decrease (compare Figures 1b and 2b).

Additional simulations with progressively higher initial concentrations of phenanthrene in the absence of hexadecane show that DO concentrations eventually drop below 0.1 mg/l and remain low until most of the phenanthrene has been metabolized indicating that biodegradation becomes limited by oxygen availability (data not shown). However, the simulations also show that DO concentrations can be increased to near saturation concentration levels by increasing the aeration rate coefficient and/or increasing oxygen saturation concentrations. This could be done by bubbling air through the water phase and/or by using oxygen enriched air.

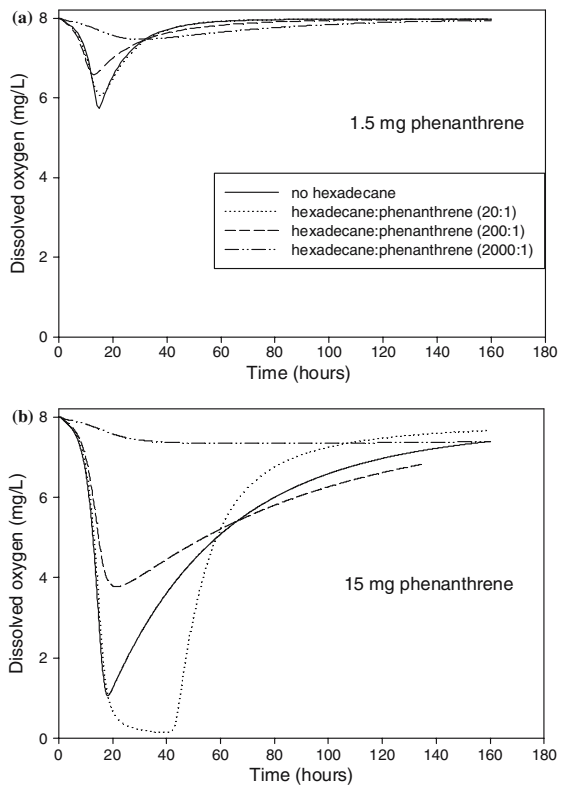

Figure 2. Model simulations of DO as a function of time during phenanthrene mineralization in the presence and absence of a hexadecane NAPL phase.

Phenanthrene bioavailability

As shown in Equation 7, the aqueous phase phenanthrene concentration (C_1) as a function of time is calculated from the time-dependent changes in the dissolution of the solid phase, partitioning, and biodegradation. Initial concentrations of C_1 were arbitrarily set to 0.0001 mg/l in all cases (Table 2). In the absence of NAPL, C_1 increased to saturation concentrations (1.12 mg/l) within the first few hours due to solubilization (Figure 3a, b) . However, following the onset of biodegradation, C_1 then decreased by 2–3 orders of magnitude during the next 10 to 15 h. In the presence of NAPL, maximum C_1 values never reached more than 1–3 orders of magnitude lower than saturation and showed a steady decrease even after the first 20 h of the simulation (Figure 3a, b). Detailed analysis of the data shows that the low C_1 values in the presence

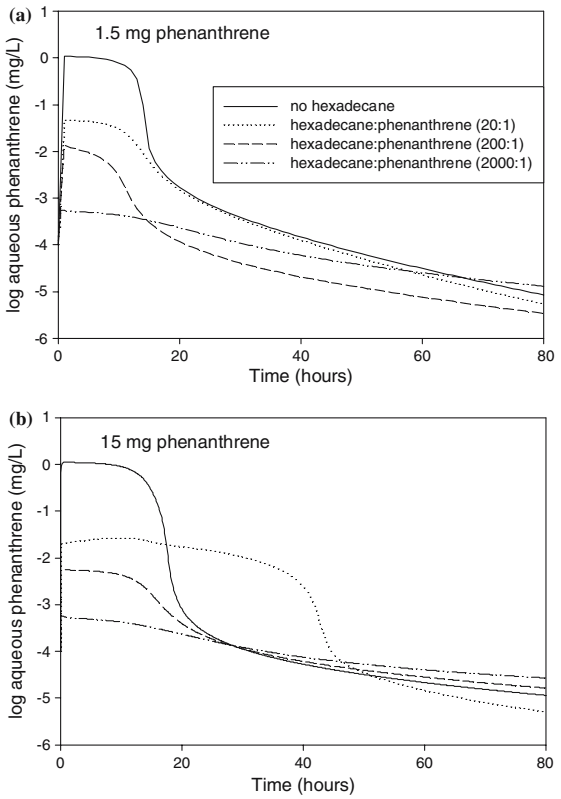

Figure 3. Model simulations of the aqueous phase concentration of phenanthrene as a function of time during phenanthrene mineralization in the presence and absence of a hexadecane NAPL phase.

of hexadecane are due to partitioning of phenanthrene into the NAPL phase. However, the slow to rapid decrease in C_1 following onset of biodegradation is the result of exponential accumulation of cell mass and the attendant rapid increase in utilization of aqueous phase phenanthrene. The model calculated values of C_1 are useful in defining the water phase concentration of phenanthrene that is required to support active biodegradation and to examine the quantitative effects of changing C_1 on rates of biodegradation. Possible approaches for increasing C_1 in the presence of NAPL so that the rate of biodegradation could be enhanced are discussed below.

Phenanthrene distribution

BRKNAPL allows specifying the initial distribution of phenanthrene between the solid phase, $Cxs_{1,\text{initial}}$, and the NAPL phase, $C_{1,\text{NAPL, initial}}$. As the aqueous phase phenanthrene (C_1) is degraded, it is replenished by dissolution of the solid phase or by departioning from the NAPL phase. The respective changes in concentration of C_1, Cxs_1, and $C_{1,\text{NAPL}}$ that are calculated by the model depend on the specified values of: (i) the coefficient kL_1 which defines the rate of dissolution of the solid phase, (ii) $kc_{1,\text{NAPL}}$, which describes rates of partitioning in/out of the hexadecane phase, and (iii) the overall kinetics of aqueous phase phenanthrene degradation.

Simulations where all of the phenanthrene is initially present as a solid phase are shown in Figures 4 and 5. These simulations show that increasing kL_1 accelerates disappearance of solid phase phenanthrene (Cxs_1) but also increases the concentration of phenanthrene in the NAPL phase (C_{NAPL}) (Figure 4a). The impact of increasing kL_1 from 100 to 200 on biodegradation (CO_2 production) is small as shown by a progressively slower mineralization as more of the phenanthrene partitions into the hexadecane phase (Figure 4b). Increasing kL_1 further to 500 caused a more pronounced decrease in mineralization because higher rates of solubilization result in accumulation of the phenanthrene in the NAPL phase. Further simulations show that even lower rates of mineralization occur under the initial condition that all the phenanthrene is in the NAPL phase (data not shown).

Another set of simulations were conducted to examine the effect of changing the rate of phenanthrene partitioning/departitioning. For these simulations, the assumption was made that all phenanthrene was initially present in the NAPL phase (both kL_1 and $Cxs_{1,\text{ initial}}$ were set to zero) which means that the departitioning rate ($kc_{1,\text{NAPL}}$) controls the aqueous phase phenanthrene (C_1). Increasing the value of $kc_{1,\text{NAPL}}$ from 20 to 100 increased the rate of mineralization throughout the whole test but further increasing it from 100 to 200 had essentially no effect (Figure 5). Increasing the value $kc_{1,\text{NAPL}}$ results in a more rapid transfer of NAPL-partitioned phenanthrene into the water phase resulting in higher aqueous phase phenanthrene concentrations (C_1) hence increasing bioavailability. The finding that departitioning can limit rates of mineralization has important practical implications in the application of bioremediation technologies. If departitioning is the rate-limiting factor, one possible approach is to increase the

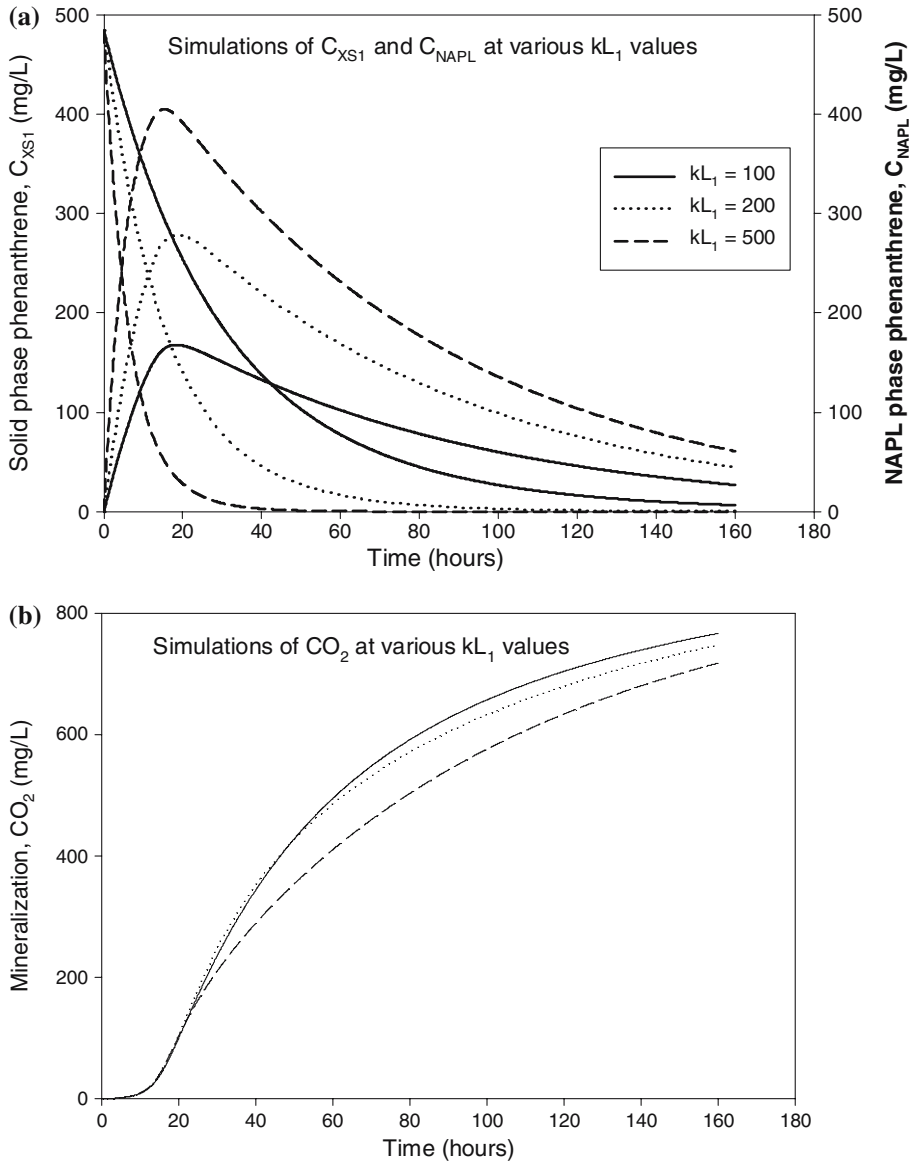

Figure 4. Model simulations of the effect of varying the phenanthrene (15 mg) dissolution rate from the solid phase (kL_1) on (a) solid phase phenanthrene (Cxs_1), exponential curves, and NAPL phase phenanthrene ($C_{1,NAPL}$), parabolic curves, as a function of time during phenanthrene mineralization. (b) Impact of varying the phenanthrene dissolution rate from the solid phase (kL_1) on mineralization.

interfacial area between the water and hexadecane phases by either (a) physically mixing the two phases, or (b) creating thin film flow environments. Another possibility is to increase solubility of phenanthrene in water relative to hexadecane using surfactants or cosolvents. In effect, this increases the value of Cxs_1 in Equation 6 and results in more favorable conditions for mass transfer to the water phase.

Conclusions

The combination of batch reactor testing and mathematical modeling described in this research has allowed development of mechanistic and quantitative descriptions of how the presence of a NAPL phase can affect biodegradation of solid phase phenanthrene. Our findings indicate that a NAPL phase can impact the biodegradation of a

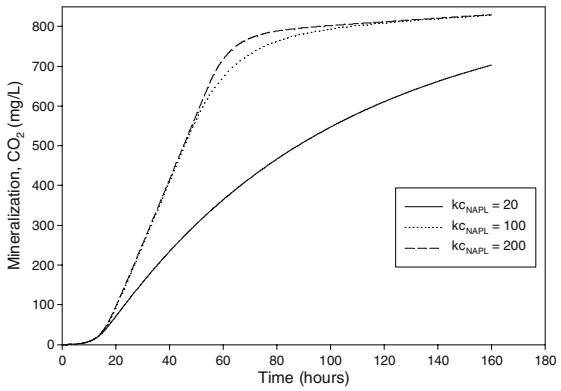

Figure 5. Model simulations of the effect of varying the de-partitioning rate ($kc_{1,NAPL}$) on phenanthrene (15 mg) mineralization.

solute such as phenanthrene via several mechanisms including those suggested in previous studies, namely, reduction in oxygen tension (Morrison & Alexander 1997) and limiting PAH bioavailability (Efroymson & Alexander 1994, 1995) as well as physiological effects resulting in different ratios of cell mass yields and CO_2 production.

Our findings indicate that at low NAPL:phenanthrene ratios, the dominant effect is that the *rate* of phenanthrene mineralization is increased. With 15 mg phenanthrene, aqueous phenanthrene concentrations in the 20:1 hexadecane:phenanthrene treatment were greater than those in all other treatments from ca. 20 to 40 h (Figure 3b). Interestingly, the model simulations indicate that with 15 mg phenanthrene, the rate of mineralization was constrained by anoxic conditions during the periods of exponential growth that occurred during hours 20 to 40 (Figure 2b). In contrast to the stimulatory effects observed in treatments containing low NAPL:phenanthrene mass ratios, high NAPL:phenanthrene mass ratios cause the *rate* of mineralization to be slowed. Modeling results indicate that this is because the aqueous phase phenanthrene concentration is reduced as the NAPL mass is increased (Figure 3). This can have a large impact on biodegradation rates as illustrated by the data from the NAPL:phenanthrene mass ratio of 2000:1 (Figure 1b).

Model studies suggest that rates of biodegradation can be increased by modifying selected physical and chemical conditions that control biodegradation in multiphase systems, namely, PAH bioavailability (e.g., aqueous phase phenanthrene) and terminal electron acceptor availability (e.g., dissolved oxygen). With respect to phenanthrene bioavailability, model simulations suggest that: (i) increasing the interfacial area between the aqueous and solid phases, (ii) increasing the rate of phenanthrene solubilization, and (iii) minimizing the accumulation of phenanthrene in the NAPL phase will result in significantly higher rates of biodegradation. Possible approaches to increasing phenanthrene bioavailability will depend on the system in question. However, any approach that either increases the physical mixing of the NAPL and aqueous phases or that increases the solubility of phenanthrene in the aqueous phase will result in increased biodegradation. Such approaches include the addition of surfactants or cosolvents (to increase solubility), aeration, or hydraulic pulsing, to increase mixing of the two phases. With respect to terminal electron acceptor availability, under conditions where DO become limiting, simulations indicate that increasing the re-aeration rate coefficient and/or increasing oxygen saturation concentrations through the addition of pure oxygen rather than air should result in enhanced biodegradation rates. Further quantitative investigations into effects of NAPL phases on PAH biodegradation in more complex systems containing soil and multiple microbial populations are warranted to develop additional strategies to enhance *in situ* biological treatment technologies of contaminated soils.

Acknowledgements

This research was supported in part by grant 2 P42 ESO4940-11 from the National Institute of Environmental Health Sciences, NIH, and in part by grant CHE-0133237 from the National Science Foundation.

References

Al-Tahhan R, Sandrin TR, Bodour AA & Maier RM (2000) Rhamnolipid-induced removal of lipopolysaccharide from *Pseudomonas aeruginosa*: effect on cell surface properties and interaction with hydrophobic substrates. Appl. Environ. Microbiol. 66: 3262–3268

Birman I & Alexander M (1996) Optimizing biodegradation of phenanthrene dissolved in nonaqueous-phase liquids. Appl. Microbiol. Biotechnol. 45: 267–272

Carroquino MJ & Alexander M (1998) Factors affecting the biodegradation of phenanthrene initially dissolved in different nonaqueous-phase liquids. Environ. Toxicol. Chem. 17: 265–270

Doick KJ & Semple KT (2003) The effect of soil:water ratios on the mineralization of phenanthrene:LNAPL mixtures in soil. FEMS Microbiol. Lett. 220(1): 29–33

Efroymson RA & Alexander M (1994) Role of partitioning in biodegradation of phenanthrene dissolved in nonaqueous-phase liquids. Environ. Sci. Technol. 28: 1172–1179

Efroymson RA & Alexander M (1995) Reduced mineralization of low concentrations of phenanthrene because of sequestering in nonaqueous phase liquids. Environ. Sci. Technol. 29: 515–521

Fu MH & Alexander M (1995) Use of surfactants and slurrying to enhance the biodegradation in soil of compounds initially dissolved in nonaqueous-phase liquids. Appl. Microbiol. Biotechnol. 43: 551–558

Gamerdinger AP, Achin RS & Traxler RW (1995) Effect of aliphatic nonaqueous phase liquids on naphthalene biodegradation in multiphase systems. J. Environ. Qual. 24: 1150–1156

Garcia-Junco M, De Olmeda E & Ortega-Calvo JJ (2001) Bioavailability of solid and non-aqueous phase liquid (NAPL)-dissolved phenanthrene to the biosurfactant-producing bacterium *Pseudomonas aeruginosa* 19SJ. Environ. Microbiol. 3(9): 561–569

Jahan K, Ahmed T & Maier WJ (1999) Modeling the influence of nonionic surfactants on biodegradation of phenenanthrene. Water Res. 33: 2181–2193

Jimenez IY & Bartha R (1996) Solvent-augmented mineralization of pyrene by a *Mycobacterium* sp. Appl. Environ. Microbiol. 62: 2311–2316

Kanaly RA, Bartha R, Watanabe K & Harayama S (2000) Rapid mineralization of benzo[*a*]pyrene by a microbial consortium growing on diesel fuel. Appl. Environ. Microbiol. 66(10): 4205–4211

Kanaly RA, Bartha R, Watanabe K & Harayama S (2001) Enhanced mineralization of benzo[*a*]pyrene in the presence of nonaqueous phase liquids. Environ. Toxicol. Chem. 20: 498–501

Kohler A, Schuttoff M, Bryniok D & Knackmuss HJ (1994) Enhanced biodegradation of phenanthrene in a biphasic culture system. Biodeg 5: 93–103

Labare MP & Alexander M (1995) Enhanced mineralization of organic compounds in nonaqueous phase-liquids. Environ. Toxicol. Chem. 14: 257–265

Marinucci AC & Bartha R (1979) Apparatus for monitoring the mineralization of volatile ^{14}C-labeled compounds. Appl. Environ. Microbiol. 38: 1020–1022

Morrison DE & Alexander M (1997) Biodegradability of nonaqueous-phase liquids affects the mineralization of phenanthrene in soil because of microbial competition. Environ. Toxicol. Chem. 16: 1561–1567

Ortega-Calvo JJ, Birman I & Alexander M (1995) Effect of varying the rate of partitioning of phenanthrene in nonaqueous-phase liquids on biodegradation in soil slurries. Environ. Sci. Technol. 29: 2222–2225

Papageorgakopoulou H & Maier WJ (1984) A new modeling technique and computer-simulations of bacterial growth. Biotechnol. Bioeng. 26: 275–284

Prabhu Y & Phale PS (2003) Biodegradation of phenanthrene by *Pseudomonas* sp strain PP2: novel metabolic pathway, role of biosurfactant and cell surface hydrophobicity in hydrocarbon assimilation. Appl. Microbiol. Biotechnol. 61: 342–351

Woo SH & Rittman BE (2000) Microbial energetics and stoichiometry for biodegradation of aromatic compounds involving oxygenation reactions. Biodegradation 11: 213–227

Zhang Y, Maier WJ & Miller RM (1997) Effect of rhamnolipids on the dissolution, bioavailability and biodegradation of phenanthrene. Environ. Sci. Technol. 31: 2211–2217

Zhang Y & Miller RM (1994) Effect of a *Pseudomonas* rhamnolipid biosurfactant on cell hydrophobicity and biodegradation of octadecane. Appl. Environ. Microbiol. 60: 2101–2106